Low-temperature phase segregation in La$_{2/3}$Ba$_{1/3}$MnO$_3$: Manifestation of nonequilibrium thermodynamics

A.B. Beznosov, E.L. Fertman, and V.A. Desnenko

B. Verkin Institute for Low Temperature Physics and Engineering of the National Academy of Sciences of Ukraine,
47 Lenin Ave., Kharkov 61103, Ukraine
E-mail: beznosov@ilt.kharkov.ua

A. Feher and M. Kajňaková

Centre of Low Temperature Physics of the Faculty of Science of P.J. Šafárik University and IEP SAS, Park Angelinum 9,
SK-04154 Košice, Slovakia

C. Ritter

Institut Laue-Langevin, Boite Postale 156, 38042 Grenoble Cedex 9, France

D. Khalyavin

Institute of Solid State and Semiconductor Physics NASB, 17 P. Brovka str., 220072 Minsk, Belarus

Thermodynamic characteristics of the perovskite-like compound La$_{2/3}$Ba$_{1/3}$MnO$_3$ exhibiting structural phase transformation of the martensitic type with characteristic temperature $T_s \approx 200$ K have been studied in the temperature range 2–340 K. Step-like hysteretic temperature behavior of the effective heat capacity has been revealed at 150–250 K and attributed to the discrete kinetics and a latent heat of the martensitic transformation. Magnetic subsystem was found exhibiting magnetic glass state below 220 K and temperature hysteresis of the magnetic susceptibility brightly pronounced in the 40–100 K and 180–230 K regions. The Debye and Einstein temperatures, $\theta_D = 230$ K and $\theta_E = 500$ K, respectively, derived from the experimental Debye–Waller factors for La/Ba, Mn and O sublattices, have been used to refine contributions from the structural and magnetic transformations to the heat capacity and to reveal thermodynamically nonequilibrium states.

1. Introduction

Low-temperature phase segregation is characteristic feature of the perovskite-like complex manganese oxides [1]. As it was recently shown [2], structural segregation in manganites develops due to the martensitic transformations (MT). The MT is a first-order diffusionless structural transformation that generally occurs between a high-temperature parent phase (austenite) and a low-temperature phase with a lower symmetry (martensite). The transformation proceeds via an atomic rearrangement that

involves a collective shear displacement. It is accompanied by the self-organized development of the phase segregated state in a wide temperature range, when the high temperature crystal phase and the low temperature one coexist. On cooling the growing low temperature phase applies stress to the other regions of the same crystallite (so-called accommodation strains), preventing them from transformation. Further cooling is needed for a further growing of the martensitic phase. The properties of such compounds are strongly dependent on the history of the material and experimental details [2,3]. The MT is

widely encountered in nature, with examples being observed in cuprate superconductors [4], transition metal alloys [5], actinides [6], colossal magnetoresistance manganites [2,7–9]. They govern unique properties of the compounds, such as the shape-memory effect in intermetallic compounds [10], unusual stepwise magnetic relaxation [3,11] and the huge value of magnetoresistance [2] in manganites. The last effect stems from a combination of the long-range deformations of the crystal lattice (accommodation strains) and the effects of strong electron correlation [2]. MT in CMR perovskite manganites leads to the self-organized strain-induced nanometer-scale to sub-μm-scale phase coexistence [2,7,12]. Martensitic transformations revealed in the narrow-band CMR manganites are tightly connected with the charge ordering phenomena and lead to the hole undoped antiferromagnetic (AFM) and the hole rich ferromagnetic (FM) phase coexistence [2,13,14]. In wide band CMR manganites the structural transformations are often considered a secondary effect and less studied. Meanwhile, in $La_{2/3}Ba_{1/3}MnO_3$ the martensitic phase transformation in the vicinity of 200 K leads to a structural phase segregated state of the compound below room temperature, determining its characteristic properties. Among them there are the huge temperature hysteresis of magnetization and ultrasound properties, the giant anomaly of magnetic susceptibility under low uniaxial pressure [8], stepwise temperature behavior of the magnetic susceptibility and the corresponding singular behavior of the internal friction [15]. The last phenomena reflect the specific relaxation phenomena caused by the discrete martensitic kinetics. It has to be mentioned, that the similar hysteretic behavior earlier reported for the low temperature structural phase transformations in the wide-band CMR manganites $La_{0.8}Ba_{0..2}MnO_3$ [16,17], $La_{0.825}Sr_{0.175}MnO_3$ [18,19] and $La_{0.80}Sr_{0.20}MnO_3$ [18,20], permits to assume the martensitic nature of these transformations. Contrary to the martensitic transformations in the narrow band manganites reported, the MT in $La_{2/3}Ba_{1/3}MnO_3$ occurs in the ferromagnetic state and leads to the coexistence of two ferromagnetic phases with equal electronic density: the rhombohedral $R\bar{3}c$ (austenite) and the orthorhombic *Imma* one (martensite).

2. Experiment

Here we use heat capacity and magnetic susceptibility measurements to gain insight into the nature of the martensitic phase transition in wide band manganites. A polycrystalline $La_{2/3}Ba_{1/3}MnO_3$ was studied. The samples were cut from ceramic pellets of the $La_{2/3}Ba_{1/3}MnO_3$ compound which were prepared using standard solid-state reaction with stoichiometric amounts of powders of La_2O_3, $BaCO_3$, and Mn_2O_3; the details are similar to

those published in Ref. 8. The sample quality was confirmed by x-ray diffraction study.

Heat capacity measurements were made using Quantum Design Physical Properties Measurement System (PPMS) in cooling and heating mode in the 2–250 K temperature range. In order to ensure that the martensitic system had reached the quasi equilibrium state [21] it was allowed to stabilize for around one hour at each temperature. Long stabilization times at each T point at a pinning of the structure domains boundaries to defects in the system [22,23]. The dc magnetization M_N (and the effective magnetic susceptibility $\chi_N = M_N/H$) of the $La_{2/3}Ba_{1/3}MnO_3$ sample were measured in the temperature range 4–320 K in the external magnetic field $H = 20$ Oe by means of a SQUID magnetometer. The sample size was 3.13×2.39×3.14 mm, and the demagnetization factor, respectively, was $N \approx 5$ in the long side direction, along which the external magnetic field was applied. The effective inner field in the sample was ~0.4 Oe. Neutron diffraction data in the 5–370 K temperature range were obtained using the D2B diffractometer of the Institute Laue-Langevin at a wavelength of $\lambda = 1.594$ Å (the details of the experiment are the same as those in Ref. 8).

3. Results and discussion

The «effective heat capacity» value $C^*(T)$ (Fig. 1,*a*) as measured by PPMS represents the sum of the heat capacity of the compound and the accompanying contribution caused by a latent heat of the first order (martensitic) phase transition (including shift energy of the structural domain boundaries).

The $C^*(T)$ data show an unusual non-regular step-like behavior in the region of martensitic phase transformation around $T_s \approx 200$ K (Fig. 1,*b*). It coordinates with stepwise temperature behavior of the magnetic susceptibility and corresponding singular behavior of the internal friction in the $R\bar{3}c \leftrightarrow Imma$ transformation region which were found recently in the studied compound [15]. Such a kinetics is typical for reversible martensitic transformations, when the macroscopic strain discontinuity splits into a set of bursts corresponding to transitions between neighboring metastable states [24]. It has to be noted, that martensitic structure develops as a result of a serial stepwise transformations of a microstructure, description of which require exploiting of methods of the nonequilibrium thermodynamics [25]. Elementary acts of the cooperative chain displacements of the coherent martensitic boundary, which proceed with a velocity of order of the sound one, represent characteristic feature of MT. Microscopic theory of the phenomenon is based on the laser mechanism of MT, according to which diffusionless rearrangement of a structure is provided by a coherent coupling of atoms due to the spontaneous emission of the phonons by the system, previously transferred into a
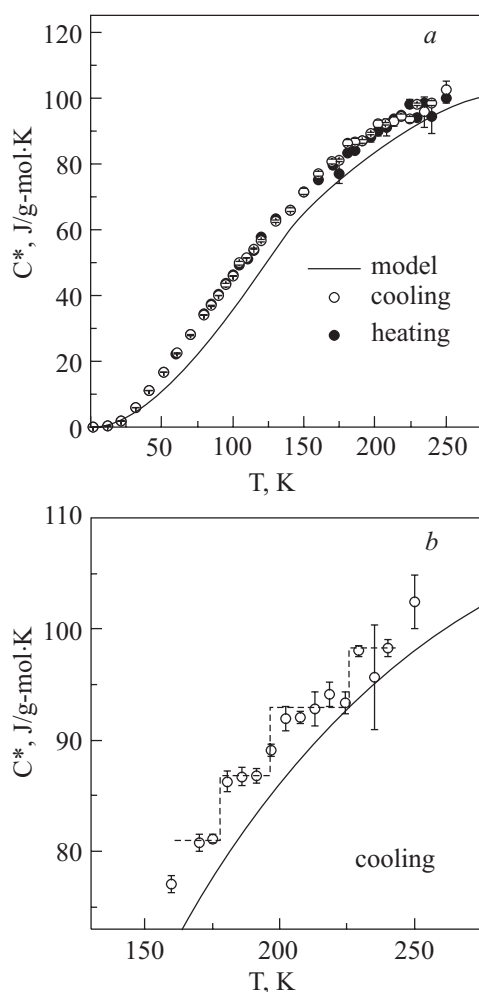
Fig. 2. Alternating temperature hysteresis of the «effective heat capacity» C*(T) of La$_{2/3}$Ba$_{1/3}$MnO$_3$ as difference of the data of cooling and following heating processes.

Fig. 1. Temperature dependent «effective heat capacity» C*(T) of La$_{2/3}$Ba$_{1/3}$MnO$_3$ in cooling and heating mode (*a*). Stepwise behavior of C*(T) in the structural transformation region (the dotted line is a guide for eyes). The solid lines represent the model Debye–Einstein heat capacity (*b*).

nonequilibrium state. So, MT is not thermodynamic, but kinetic transition of the system «atoms+phonons» far from an equilibrium [21]. Thus, Fig. 1,*b* clearly reflects effects of such transitions on the cooling and heating processes in the system.

Another characteristic feature of the phenomenon observed is an alternating hysteresis of the C*(T) curves has been revealed above 50 K on cooling and heating (Fig. 2). The hysteretic behavior of the «effective heat capacity» found is consistent to that of the magnetic susceptibility χ_N above 40 K (Fig. 3). Below 40 K C*(T) curves show no hysteresis within the experimental error. The hysteretic C*(T) loop does not converge at 250 K. This can be considered as an evidence of the incomplete reverse martensitic transition.

Significant uncertainty of the experimental data (characterizing nonequilibrium state of the system) is seen in the martensitic transformation region (Figs. 1,*b*, 2). This
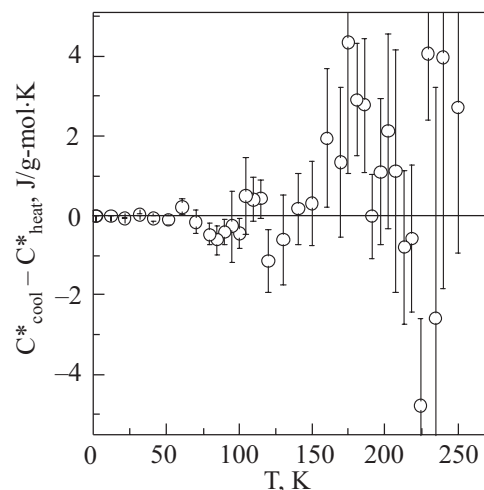
is in a good agreement with [23,26]: as passing through a first order transition, the sample should emit latent heat, producing a PPMS decay curve that cannot be well modeled by the analysis software. PPMS uses the thermal-relaxation method based on the assumption that the sample specific heat does not vary over the temperature range encompassed by a decay cycle. This will be true only when the relative change in the heat capacity over the temperature span ΔT is small. In the phase transition region the relative change in the sample heat capacity with temperature can be large, which renders this assumption invalid. A decay cycle consists of the establishment of steady state at a temperature $T_0 + \Delta T$ (T_0 is the thermostat temperature, $\Delta T \sim 0.02$–0.2 K) followed by relaxation to T_0. The time dependent temperature $T(t)$ of the sample can be described as follows

$$T(t) = T_0 + \Delta T \exp\left(-\frac{t}{\tau}\right), \tag{1}$$

where τ is a thermal relaxation time. An extended series of decays cycles (10–100) has been averaged at each temperature to produce heat-capacity measurements that have a minimal point-to-point scatter depending on the temperature region.

Temperature dependences of the decay time τ were found to be anomalous (jump-like) above 50 K (Fig. 4). Such a peculiar character of the $\tau(T)$ dependences in the martensitic transformation region reflects a latent-heat contribution associated with discontinuous burst-like martensitic kinetics (the discrete process of the $R\bar{3}c \leftrightarrow Imma$ phases exchange exists in La$_{2/3}$Ba$_{1/3}$MnO$_3$ in a wide temperature interval around T_s [8,15]).

A similar non-regular behaviour of the temperature dependent heat capacity curves has been found in the shape-memory In-Tl alloy in the martensitic phase trans-
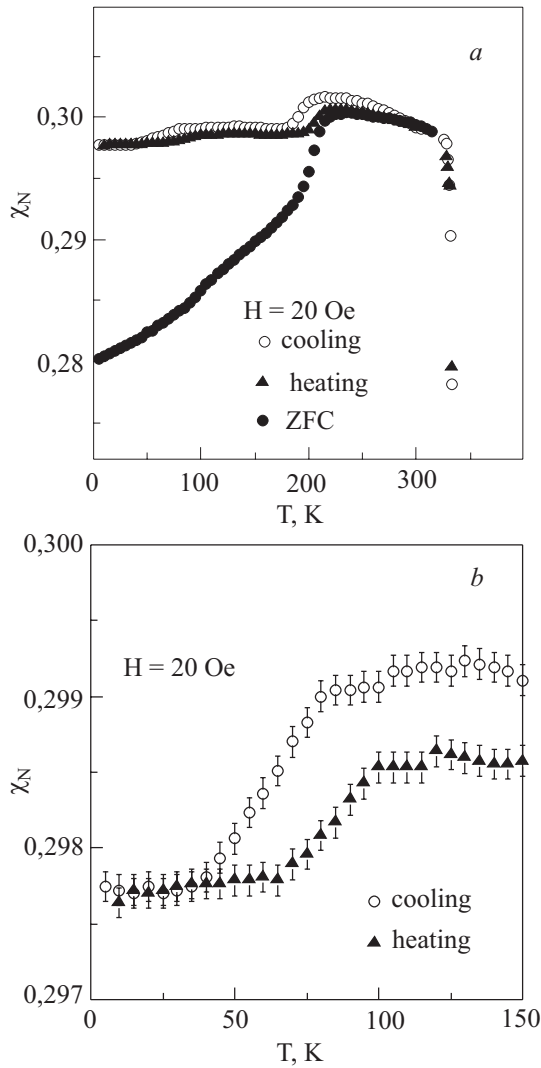
Fig. 4. Temperature dependence of the thermal relaxation time τ (PPMS) of the La$_{2/3}$Ba$_{1/3}$MnO$_3$ sample on cooling and heating.

Fig. 3. Temperature dependence of the effective magnetic susceptibility χ$_N$ of La$_{2/3}$Ba$_{1/3}$MnO$_3$ in the external magnetic field 20 Oe at the field cooled and zero field cooled (ZFC) regimes (*a*); the 40–100 K hysteresis region (*b*).

formation region (Fig. 2 in [27]). It may be a common feature of the temperature dependence of the effective heat capacity of martensitic compounds in the vicinity of MT.

The temperature dependent magnetic susceptibility χ$_N$(T) curves of La$_{2/3}$Ba$_{1/3}$MnO$_3$ are strongly hysteretic below the room temperature (Fig. 3). As one can see in Fig. 3,*b*, there is an «additional» (to that between ∼180 K and ∼230 K [8,15]) pronounced temperature hysteresis of the magnetic susceptibility in the 40–100 K region, which implies a first order transition which was not reported earlier.

Beside the difference between curves measured on heating and cooling there is a strong difference between the field cooled (FC) curves and zero field cooled ones (ZFC), which is typical for a cluster glass state. A similar behavior was previously reported for many phase segregated manganites close to a first-order electronic phase
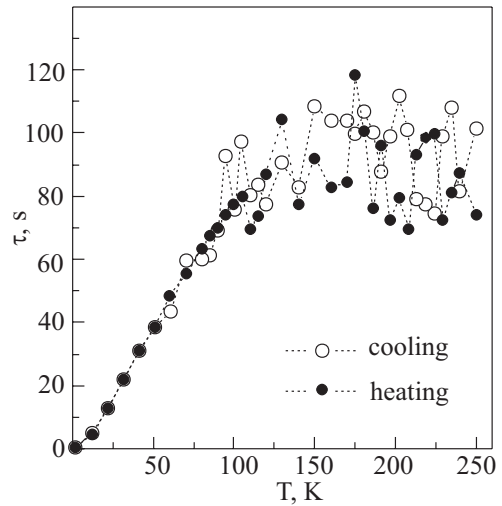
transitions [11,28]. The origin of the spin-glass-like characteristics is usually ascribed to the frustration introduced by the competition between ferromagnetic-double exchange and antiferromagnetic-superexchange. In our case, below room temperature clusters of two ferromagnetic phases possessing different crystal structures are coexisting in different proportions due to the martensitic phase transition in the vicinity of 200 K [8]. The clusters are evidently interdependent by the martensitic accommodation stresses. Characteristic glassy behavior and accompanying relaxation phenomena (memory, aging, etc.) can be perfectly understood taking into account only the intercluster interactions [28].

One more peculiarity can be seen in the magnetic curves in the 100 K region (Fig. 3,*a*): a change of the slope of the ZFC χ$_N$(T) curve which seems to be connected with the above mentioned «additional» temperature hysteresis (Fig. 3,*b*) of the magnetic susceptibility in the low magnetic field 20 Oe. The change of the slope mentioned implies a decreasing of the number of the ferromagnetically ordered ions in the system. More complete description of the phenomenon requires a special research.

In order to make this low temperature anomaly visible on the heat capacity curves as well the background was subtracted from the data for the last ones. The «pure lattice» heat capacity data (i.e. ones which do not include the phase transition and magnetic contributions, and so can be considered as certain background) were fitted using an equation of the form

$$C_{\text{mod}}(T) = C_D(T) + C_E(T), \qquad (2)$$

where $C_D(T)$ and $C_E(T)$ are the Debye's and Einstein's contributions, respectively:

$$C_D(T) = 0.2C_{cl}3\left(\frac{T}{\theta_D}\right)^3\int_0^{\frac{\theta_D}{T}}\frac{x^4e^x dx}{(e^x-1)^2}, \qquad (3)$$

$$C_E(T) = 0.8C_{cl}\frac{\theta_E^2 e^{\frac{\theta_E}{T}}}{T^2\left(e^{\frac{\theta_E}{T}}-1\right)^2}. \qquad (4)$$

Both characteristic temperatures (the Debye temperature θ_D and the Einstein temperature θ_E) have been found from the experimental values of temperature dependent Debye–Waller factors $B(T)$ (Fig. 5), obtained from the neutron diffraction data and fitted using the equations Eqs. (5)–(7) [29,30]:

$$B_{Mn}(T) \approx A_D\frac{T^2}{\theta_D^3}\int_0^{\frac{\theta_D}{T}}\coth\left(\frac{x}{2}\right)x dx, \qquad (5)$$
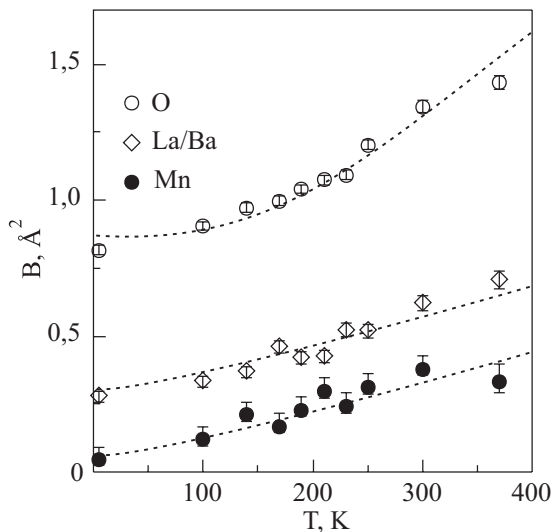

Fig. 5. Temperature dependent Debye–Waller factors $B(T)$ of Mn, La/Ba and O in La$_{2/3}$Ba$_{1/3}$MnO$_3$ compound obtained from neutron diffraction data. The dashed lines are approximations of the data by the Eqs. (5)–(7).

$$B_{La/Ba}(T) \approx B_s + A_D\frac{T^2}{\theta_D^3}\int_0^{\frac{\theta_D}{T}}\coth\left(\frac{x}{2}\right)x dx, \qquad (6)$$

$$B_O(T) \approx \frac{A_E}{\theta_E}\coth\frac{\theta_E}{2T}. \qquad (7)$$

Here $B_{Mn}(T)$, $B_{La/Ba}(T)$ and $B_O(T)$ are experimental temperature dependent values of Debye–Waller factors for Mn, La(Ba) and O, correspondingly; $A_D = 29$ Å^{2}K, $A_E = 445$ Å^{2}K and $B_s = 0.237$ Å^2 are fitting parameters (B_s is a static contribution to the Debye–Waller factor caused by the chemical disorder in the La/Ba lattice sites), obtained by the least-squares method.

We have found that in the studied temperature region 2–250 K a set with an acoustical mode of characteristic energy parameter $\theta_D = 230$ K and an optical mode with $\theta_E = 500$ K fit the «lattice background» (lattice heat capacity without contributions from magnetic subsystem and structural phase transitions) fairly well (Fig. 1). The classical heat capacity is $C_{cl} = 3R\nu$, R is the universal gas constant, and $\nu = 5$ is the number of atoms in the formula unit of the compound. The coefficients 0.2 and 0.8 reflect weights of the three translation degrees of freedom of the formula unit and the twelve internal oscillatory ones, correspondingly*.

It has to be mentioned that the Debye temperature obtained $\theta_D = 230$ K is much lower then ones being in use sometimes. For example the value $\theta_D \approx 400$ K is obtained in the paper Ref. 31 using the low temperature data from 2–8 K region and Debye heat capacity

$$C(T) = C_{cl}3\left(\frac{T}{\theta_D}\right)^3\int_0^{\frac{\theta_D}{T}}\frac{x^4e^x dx}{(e^x-1)^2}$$

in the low temperature limit for the lattice contribution. However value $\theta_D = 400$ K being substituted into this equation permits neither to fit the temperature dependent heat capacity in the wide temperature range (and leads to the C_D value substantially exceeding the experimental $C^*(T)$ data between 50 K and 250 K), nor to fit the experimental temperature dependent Debye–Waller factors $B(T)$ by Eqs. (5)–(7).

---

* Oscillations of crystal lattice can be presented as oscillations of the unit cell as a whole (acoustical modes), and internal oscillations in the unit cell (optical modes). Oscillations of the formula units as a whole inside unit cells are determined by the same elastic modules, as the oscillations of the unit cells (chemical bonds between unit cells are the same as between formula units). So, it is reasonable to ascribe an acoustical spectrum to the formula units' oscillations at a simplified approach, and to ascribe an optical spectrum to the internal oscillations of the formula units. Taking into account, that complete number of the degrees of freedom per formula unit is 15, three of which are translational ones (i.e. correspond to acoustical oscillations) and 12 degrees of freedom correspond to optical oscillations, we get relation 0.2 to 0.8 for the corresponding contributions to the heat capacity per formula unit (or mole).

The temperature dependence of the heat capacity data where the lattice contribution has been subtracted (Fig. 6) clearly shows two anomalous regions: the martensitic one around 200 K and the low temperature one below 100 K. The last one is evidently connected with the magnetic anomaly (see Fig. 3), nature of which requires an additional study. It is clear, however, that the decreasing of the magnetization observed reflects an increasing of antiferromagnetic order parameter in certain regions inside of the structural domains or in the border layers between them (problem of determination of the character of the magnetic structure of $La_{2/3}Ba_{1/3}MnO_3$ is discussed in [8]).

Comparing the temperature dependence of the entropy, as calculated using the experimentally determined effective heat capacity
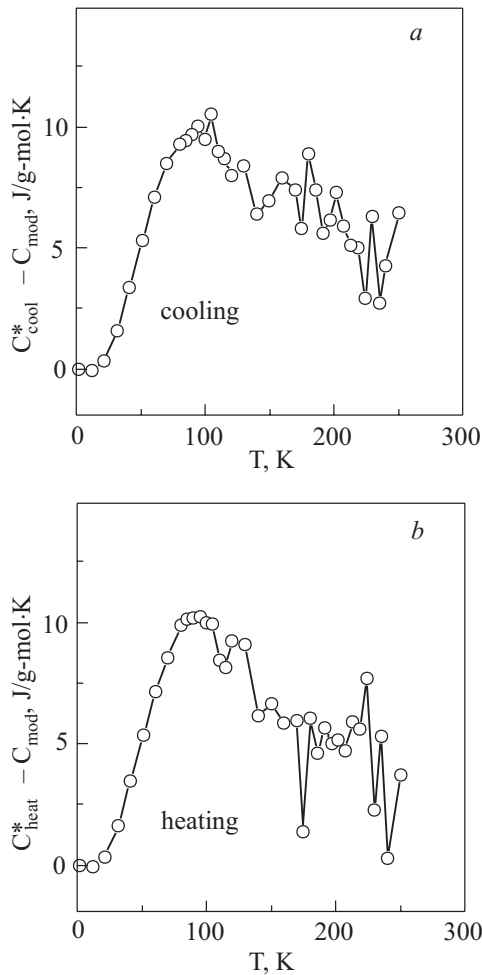
$$S(T) = \int_0^T \frac{C^*(x)}{x} dx,$$

with the model dependence

$$S_{\mathrm{mod}}(T) = \int_0^T \frac{C_{\mathrm{mod}}(x)}{x} dx,$$

its very unusual behavior was revealed (Fig. 7). The two anomalous regions found, *A–B* (75–118 K) and the central martensitic transformation region *C–D* (165–237 K), are characterized by having entropy values lower than the quasiequilibrium ones. This indicates that in the phase transformation regions the steady state has not been achieved during the thermal relaxation time τ (~100 s) used in the present heat capacity experiment (Fig. 4).

4. Conclusion

In conclusion, we have studied the heat capacity and magnetic behavior of the $La_{2/3}Ba_{1/3}MnO_3$ perovskite in the phase segregated state (when two different crystal

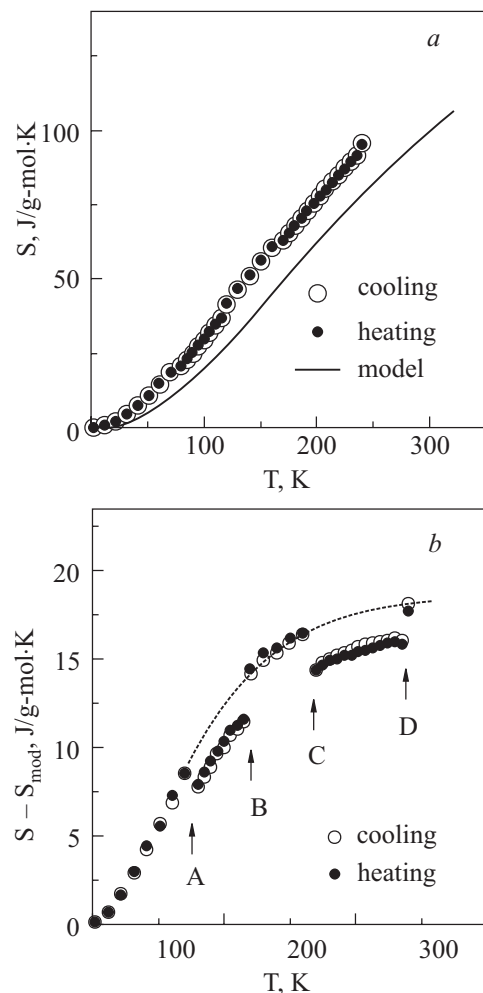*Fig. 6.* Temperature dependent «effective heat capacity» data with model lattice contribution subtracted on cooling (*a*) and on heating (*b*).

Fig. 7. Entropy of $La_{2/3}Ba_{1/3}MnO_3$ when cooling (○) and heating (●); solid line stands for the model dependence $S_{\mathrm{mod}}(T)$ (*a*). Difference between the experimental and model dependences. The *A–B* and *C–D* intervals correspond to the nonequilibrium states in the experiment. Dotted line is guide for eyes (*b*).

structures are coexistent, both being ferromagnetic), which develops due to the martensitic phase transformation below the room temperature. The temperature dependent «effective heat capacity» $C^*(T)$ was found to be hysteretic and step-like in the martensitic transformation region 150–250 K. The temperature dependent decay time τ is found to be non-regular jump-like as well. The behavior revealed reflects a latent-heat contribution associated with the discrete burst-like martensitic kinetics of the transformation. The temperature behavior of the entropy permits to conclude that the steady (i. e. thermodynamically quasiequilibrium) state is not achieved during the thermal relaxation time τ (~100 s). The lattice part of the heat capacity was modeled by the sum of the Debye and the Einstein contributions in the whole studied temperature interval 2–250 K. The Debye temperature $\theta_D = 230$ K and the Einstein temperature $\theta_E = 500$ K used have been obtained from the experimental temperature dependent Debye–Waller factors. Magnetic subsystem of the compound exhibits magnetic glass state below 220 K and «additional» temperature hysteresis of the magnetic susceptibility in the 40–100 K region.

Acknowledgements

1. E. Dagotto, *Nanoscale Phase Separation and Colossal Magnetoresistance*, Springer-Verlag, Berlin (2002).
2. V. Podzorov, B.G. Kim, V. Kiryukhin, M.E. Gershenson, and S.-W. Cheong, *Phys. Rev.* **B64**, 140406(R) (2001).
3. V. Hardy, A. Maignan, S. Hébert, C. Yaicle, C. Martin, M. Hervieu, M. R. Lees, G. Rowlands, D.McK. Paul, and B. Raveau, *Phys. Rev.* **B68**, 220402(R) (2003).
4. A.N. Lavrov, S. Komiya, and Y. Ando, *Nature* **418**, 385 (2002).
5. K. Bhattacharya, S. Conti, G. Zanzotto, and J. Zimmer, *Nature* **428**, 55 (2004).
6. G.H. Lander, E.S. Fisher, and S.D. Bader, *Adv. Phys.* **43**, 1 (1994).
7. M. Uehara and S.-W. Cheong, *Europhys. Lett.* **52**, 674 (2000).
8. A.B. Beznosov, V.A. Desnenko, E.L. Fertman, C. Ritter, and D.D. Khalyavin, *Phys. Rev.* **B68**, 054109 (2003).
9. C. Yaicle, C. Martin, Z. Jirak, F. Fauth, G. André, E. Suard, A. Maignan, V. Hardy, R. Retoux, M. Hervieu, S. Hébert, B. Raveau, Ch. Simon, D. Saurel, A. Brûlet, and F. Bourée, *Phys. Rev.* **B68**, 224412 (2003).
10. M.A. Scherling and R.W. Karz, *Shape Memory Effects in Alloys*, Plenum Pub. Corp., New York (1975).
11. T. Wu and J.F. Mitchell, *Phys. Rev.* **B69**, 100405(R) (2004).
12. Ch. Simon, S. Mercone, N. Guiblin, C. Martin, A. Brûlet, and G. André, *Phys. Rev. Lett.* **89**, 207202 (2002).
13. P.G. Radaelli, R.M. Ibberson, S.-W. Cheong, and J.F. Mitchell, *Physica* **B276-278**, 551 (2000).
14. A.B. Beznosov, E.L. Fertman, V.A. Desnenko, *Fiz. Nizk. Temp.* **34**, 790 (2008) [*Low Temp. Phys.* **34**, 624 (2008)].
15. E.L. Fertman, A.B. Beznosov, V.A. Desnenko, L.N. Pal-Val, P.P. Pal-Val, and D.D. Khalyavin, *J. Magn. Magn. Mater.* **308**, 278 (2007).
16. V. Laukhin, B. Martinez, J. Fontcuberta, and Y.M. Mukovskii, *Phys. Rev.* **B63**, 214417 (2001).
17. V.E. Arkhipov, N.G. Bebenin, V.P. Dyakina, V.S. Gaviko, A.V. Korolev, V.V. Mashkautsan, E.A. Neifeld, R.I. Zainullina, Ya.M. Mukovskii, and D.A. Shulyatev , *Phys. Rev.* **B61**, 11229 (2000).
18. E.A. Neifeld, N.G. Bebenin, V.E. Arkhipov, K.M. Demchuk, V.S. Gaviko, A.V. Korolev, N.A. Ugryumova, and Ya.M. Mukovskii, *J. Magn. Magn. Mater.* **295**, 77 (2005).
19. E.S. Itskevich, V.F. Kraidenov, and S.M. Kusmin, *Fiz. Nizk. Temp.* **32**, 1222 (2006) [*Low Temp. Phys.* **32**, 928 (2006)].
20. R.I. Zainullina, N.G. Bebinin, A.M. Burkhanov, V.V. Ustinov, and Y.M. Mukovskii, *Phys. Rev.* **B66**, 064421 (2002).
21. A.I. Olemskoi and A.A. Katsnelson, *Synergetics of Condensed Medium*, Editorial URSS, Moscow (2003), (in Russian).
22. G. Grüner, *Density Waves in Solids*, Addison-Wesley (1994).
23. S. Cox, J.C. Lashley, E. Rosten, J. Singleton, A.J. Williams and P.B. Littlewood, *J. Phys.: Condens. Matter* **19**, 192201 (2007).
24. F.-J. Pérez-Reche, L. Truskinovsky, and G. Zanzotto, *Phys. Rev. Lett.* **99**, 075501 (2007).
25. I. Prigogine and G. Nicolis, *Self-Organization in Nonequilibrium Systems*, Wiley-Interscience, N.Y. (1977).
26. J.C. Lashley, M.F. Hundley, A. Migliori, J.L. Sarrao, P.G. Pagliuso, T.W. Darling, M. Jaime, J.C. Cooley, W.L. Hults, L. Morales, D.J. Thoma, J.L. Smith, J. Boerio-Goates, B.F. Woodfield, G.R. Stewart, R.A. Fisher, N. E. Phillips, *Cryogenics* **43**, 369 (2003).
27. J.C. Lashley, R.K. Schulze, B. Mihaila, W.L. Hults, J.C. Cooley, and J.L. Smith, P.S. Riseborough, C.P. Opeil, R.A. Fisher, O. Svitelskiy, A. Suslov, and T.R. Finlayson, *Phys. Rev.* **B75**, 205119 (2007).
28. F. Rivadulla, M.A. Lypez-Quintela, and J. Rivas, *Phys. Rev. Lett.* **93**, 167206 (2004).
29. C. Kittel, *Quantum Theory of Solids*, Wiley, New York (1987).
30. J.M. Ziman, *Principles of the Theory of Solids*, Cambridge University Press, Cambridge UK (1979).
31. J. Hamilton, E.L. Keatley, H.L. Ju, A.K. Raychaundhuri, V.N. Smolyaninova, and R.L. Greene, *Phys. Rev.* **B54**, 14926 (1996).